Circulation

ORIGINAL RESEARCH ARTICLE

Restoration of Cardiac Myosin Light Chain Kinase Ameliorates Systolic Dysfunction by Reducing Superrelaxed Myosin

Tatsuro Hitsumoto, MD; Osamu Tsukamoto, MD, PhD; Ken Matsuoka, MD, PhD; Junjun Li, PhD; Li Liu, PhD; Yuki Kuramoto, MD, PhD; Shuichiro Higo, MD, PhD; Shou Ogawa, MD; Noboru Fujino, MD, PhD; Shohei Yoshida, MD, PhD; Hidetaka Kioka, MD, PhD; Hisakazu Kato, PhD; Hideyuki Hakui, MD, PhD; Yuki Saito, PhD; Chisato Okamoto, MD; Hijiri Inoue, MS; Jo Hyejin, MS; Kyoko Ueda, MS; Takatsugu Segawa, MD; Shunsuke Nishimura, MD; Yoshihiro Asano, MD, PhD; Hiroshi Asanuma, MD, PhD; Akiyoshi Tani, PhD; Riyo Imamura, PhD; Shinsuke Komagawa, PhD; Toshio Kanai, PhD; Masayuki Takamura, MD, PhD; Yasushi Sakata, MD, PhD; Masafumi Kitakaze, MD, PhD; Jun-ichi Haruta, PhD; Seiji Takashima, MD, PhD

BACKGROUND: Cardiac-specific myosin light chain kinase (cMLCK), encoded by *MYLK3*, regulates cardiac contractility through phosphorylation of ventricular myosin regulatory light chain. However, the pathophysiological and therapeutic implications of cMLCK in human heart failure remain unclear. We aimed to investigate whether cMLCK dysregulation causes cardiac dysfunction and whether the restoration of cMLCK could be a novel myotropic therapy for systolic heart failure.

METHODS: We generated the knock-in mice (*Mylk3*$^{+/fs}$ and *Mylk3*$^{fs/fs}$) with a familial dilated cardiomyopathy–associated *MYLK3* frameshift mutation (*MYLK3*$^{+/fs}$) that had been identified previously by us (c.1951-1G>T; p.P639Vfs*15) and the human induced pluripotent stem cell–derived cardiomyocytes from the carrier of the mutation. We also developed a new small-molecule activator of cMLCK (LEUO-1154).

RESULTS: Both mice (*Mylk3*$^{+/fs}$ and *Mylk3*$^{fs/fs}$) showed reduced cMLCK expression due to nonsense-mediated messenger RNA decay, reduced MLC2v (ventricular myosin regulatory light chain) phosphorylation in the myocardium, and systolic dysfunction in a cMLCK dose–dependent manner. Consistent with this result, myocardium from the mutant mice showed an increased ratio of cardiac superrelaxation/disordered relaxation states that may contribute to impaired cardiac contractility. The phenotypes observed in the knock-in mice were rescued by cMLCK replenishment through the AAV9_*MYLK3* vector. Human induced pluripotent stem cell–derived cardiomyocytes with MYLK3$_{+/fs}$ mutation reduced cMLCK expression by 50% and contractile dysfunction, accompanied by an increased superrelaxation/disordered relaxation ratio. CRISPR-mediated gene correction, or cMLCK replenishment by AAV9_*MYLK3* vector, successfully recovered cMLCK expression, the superrelaxation/disordered relaxation ratio, and contractile dysfunction. LEUO-1154 increased human cMLCK activity ≈2-fold in the V_{max} for ventricular myosin regulatory light chain phosphorylation without affecting the K_m. LEUO-1154 treatment of human induced pluripotent stem cell–derived cardiomyocytes with MYLK3$_{+/fs}$ mutation restored the ventricular myosin regulatory light chain phosphorylation level and superrelaxation/disordered relaxation ratio and improved cardiac contractility without affecting calcium transients, indicating that the cMLCK activator acts as a myotrope. Finally, human myocardium from advanced heart failure with a wide variety of causes had a significantly lower *MYLK3*/*PPP1R12B* messenger RNA expression ratio than control hearts, suggesting an altered balance between myosin regulatory light chain kinase and phosphatase in the failing myocardium, irrespective of the causes.

CONCLUSIONS: cMLCK dysregulation contributes to the development of cardiac systolic dysfunction in humans. Our strategy to restore cMLCK activity could form the basis of a novel myotropic therapy for advanced systolic heart failure.

Key Words: cardiac myosin ■ myosin light chain kinase ■ phosphorylation ■ ventricular dysfunction, left

Correspondence to: Osamu Tsukamoto, MD, PhD, Department of Biochemistry, Hyogo College of Medicine, 1-1 Mukogawa-cho, Nishinomiya, Hyogo, 663-8501, Japan. Email tsuka@medbio.med.osaka-u.ac.jp

Supplemental Material is available at https://www.ahajournals.org/doi/suppl/10.1161/CIRCULATIONAHA.122.062885.

For Sources of Funding and Disclosures, see page 1916.

Clinical Perspective

What Is New?

- The causal link between the dysregulated cardiac-specific myosin regulatory light chain kinase (cMLCK and) dilated cardiomyopathy in human cardiomyocytes was proven. The haploinsufficiency of cMLCK due to nonsense-mediated mRNA decay contributed to impaired contractility through the increasing ratio of cardiac superrelaxation/disordered relaxation states in human dilated cardiomyopathy.
- Restoration of cMLCK improved cardiac function by changing the superrelaxation/disordered relaxation ratio. Furthermore, we succeeded in developing an activator of cMLCK, which led to the development of a first-in-class treatment for heart failure.
- Human failing myocardium had relatively low activities of cMLCK compared with the control myocardium irrespective of the causes.

What Are the Clinical Implications?

- cMLCK activation successfully improved cardiac systolic function by increasing the ratio of cardiac superrelaxation/disordered relaxation states by increasing ventricular myosin regulatory light chain phosphorylation without affecting intracellular calcium transients in human induced pluripotent stem cell–derived cardiomyocytes, suggesting that cMLCK activator may potentially emerge as a new class of myotropes.
- Because failing human myocardium showed lower cMLCK activities than the control myocardium irrespective of the causes, cMLCK restoration is a potential novel myotropic strategy applicable to various types of heart failure with reduced ejection fraction.

Nonstandard Abbreviations and Acronyms

AAV	adeno-associated virus
cMLCK	cardiac-specific myosin light chain kinase
DCM	dilated cardiomyopathy
DRX	disordered relaxation
EGFP	enhanced green fluorescent protein
HFrEF	heart failure with reduced ejection fraction
iPSC-CM	induced pluripotent stem cell–derived cardiomyocyte
KI	knock-in
MLC2v	myosin regulatory light chain, ventricular/cardiac isoform
MYPT2	myosin phosphatase target subunit 2
OM	omecamtiv mecarbil
PCR	polymerase chain reaction
PP1	protein phosphatase 1
skMLCK	skeletal muscle type myosin regulatory light chain kinase
smMLCK	smooth muscle type myosin regulatory light chain kinase
SRX	superrelaxation

Myotrope is a novel class of inotrope that can enhance cardiac contraction by directly activating sarcomere proteins through a calcium-independent mechanism. By selectively activating cardiac myosin ATPase, omecamtiv mecarbil (OM), a first-in-class myotrope, improves cardiac sarcomere contractility without affecting intracellular calcium transients.[1–4] This contrasts markedly with the traditional inotropes that improve hemodynamic status at the expense of an increased risk of mortality.[2,5] OM exerted a clinically meaningful reduction in the composite end point of time to the first heart failure (HF) event or cardiovascular death among patients with severe heart failure with reduced ejection fraction (HFrEF) in the GALACTIC-HF trial (Global Approach to Lowering Adverse Cardiac outcomes Through Improving Contractility in Heart Failure).[1,3] However, the METEORIC-HF trial (Multicenter Exercise Tolerance Evaluation of Omecamtiv Mecarbil Related to Increased Contractility in Heart Failure) showed that OM did not improve exercise capacity after 20 weeks of treatment in patients with HFrEF, suggesting the need for the development of alternative myotropes.

Cardiac muscle contraction is driven through an ATP-dependent cyclic interaction between the myosin cross-bridge and actin-containing thin filaments.[6] Given the 3 major physiological modulators of sarcomeric function[5] (length-dependent activation, β_1-adrenergic signaling, and myosin regulation light chain [MLC2] phosphorylation), MLC2 phosphorylation is considered appropriate for an alternative myotrope. MLC2 wraps around the α-helical neck region of myosin heavy chain, and the phosphorylation of ventricular MLC2 (MLC2v) enhances cardiac sarcomere contractility.[7,8] Cardiac-specific overexpression of nonphosphorylatable MLC2v or decreasing MLC2v phosphorylation reduced the force generation of cardiac tissue,[9–11] and in contrast, increasing MLC2v phosphorylation enhanced the developing force.[9,12–14] In the heart, MLC2v is phosphorylated predominantly by cardiac-specific myosin light chain kinase (cMLCK), encoded by the *MYLK3* gene,[15] which is expressed exclusively in cardiomyocytes.[15,16] In contrast to smooth and skeletal muscles, in which MLC2 is phosphorylated transiently in response to brief neurostimulation, the MLC2 phosphorylation level is stable in cardiac muscles because of the continuous beating of the heart.[17] cMLCK is responsible for the maintenance of the basal phosphorylation level of MLC2v in the heart,[18,19] and its ablation results in a

marked reduction of MLC2v phosphorylation, as well as a depressed cardiac contraction with ventricular dilatation in mice and zebrafish.[15,16,18,20] We critically identified a heterozygous *MYLK3* (NM_182493.3) mutation (c.1951-1G>T) associated with human dilated cardiomyopathy (DCM),[21] although its functional consequence in vivo remains unexplored. Furthermore, MLC2v phosphorylation level was reported to reduce from 40% in healthy hearts to <18% of total MLC2v in failing human hearts,[22–24] suggesting the generality of reduced MLC2v phosphorylation in the myocardium of HFrEF.

The correction of myosin function through modulation of superrelaxation (SRX) and disordered relaxation (DRX) states of cardiac myosin has recently provided new fundamental insights into the therapeutic development for HF.[25] The total force produced by cardiac sarcomere is expressed as a product of *f* and the number of myosin heads that are bound in a force-producing state, Fe = $f \times dr \times Nt$, where *f* is the intrinsic force of each myosin head, *dr* is the duty ratio, and *Nt* is the total number of functionally available myosin heads.[8] SRX myosin heads are energy saving and unavailable for actin binding to produce force in sarcomeres and are thereby one of the key determinants of the constant *Nt*. MLC2v phosphorylation accelerates the transition from the SRX to DRX states[12,26,27] by repelling the myosin heads from the myosin filament and moving them toward the actin filament,[8] thereby increasing *Nt*. In addition, MLC2v phosphorylation increases myosin neck domain stiffness,[7] thereby increasing *f*. However, the pathophysiological and therapeutic implications of cMLCK and MLC2v phosphorylation dynamics in human HF remain unclear.

In the present study, we investigated the pathophysiological consequences of cMLCK dysregulation and investigated whether the strategy to restore cMLCK has the potential to be an alternative therapy for advanced HFrEF[27–29] by improving cardiac contractility through upregulating MLC2v phosphorylation without affecting intracellular calcium dynamics using mouse models and human induced pluripotent stem cell–derived cardiomyocytes (iPSC-CMs).

METHODS

For a detailed description of methods, please see the Supplemental Material. The data that support the findings of this study are available from the corresponding author on reasonable request.

Generation of the Mylk3 Mutant Knock-in Mice

We used the CRISPR/Cas9 technology to render the knock-in (KI) of the *Mylk3* mutant (c.1951-1G>T) in its original locus of C57BL/6 zygotes. Founders carrying the KI variant were generated by combining guide RNA, Cas9 messenger RNA (mRNA), and single-stranded oligodeoxynucleotide donors co-injected into the fertilized eggs of mice and were cross-bred according to a methodology proposed in a previous study.[30] In brief, using a micromanipulator, 100 ng/μL of Cas9 mRNA, 50 ng/μL of guide RNAs, and 50 ng/μLof single-stranded oligodeoxynucleotides of CR9 were microinjected into the pronuclei of embryos collected from superovulated C57BL/6N female mice. Injected embryos were cultured overnight, and divided 2-cell embryos were transferred into pseudopregnant C57BL/6N females. F0 mice were mated with wild-type C57BL/6N mice for germline transmission, and F1 mice were genotyped by polymerase chain reaction (PCR) using genomic DNA extracted from the tail (Expanded Methods and Materials; Figure S1; Table S2).

Generation of Human Induced Pluripotent Stem Cells and Cardiac Differentiation

Human induced pluripotent stem cells (iPSCs) were generated from peripheral blood mononuclear cells using episomal vectors, according to the protocol provided by the Center for Information on Research with Animals (Center for iPS Cell Research and Application; https://www.cira.kyoto-u.ac.jp/e/research/protocol.html). The episomal vectors were introduced into the CD34+ cells by Nucleofector 2b (Lonza) using the Amaxa Human CD34 Cell Nucleofector Kit (Lonza) and plated on cell culture plates coated with Laminin 511-E8 (iMatrix-511 silk; Nippi). After 2 weeks, colonies with iPSC-like morphologies were obtained and cultured by changing the medium with StemFit (Ajinomoto). iPSCs were differentiated into cardiomyocytes (iPSC-CMs) using an embryoid body formation protocol as described previously,[31] with slight modification using the AscleStem cardiomyocyte differentiation medium kit (Nacalai Tesque). Differentiated cardiomyocytes were purified by metabolic selection using glucose-free DMEM (Nacalai Tesque) supplemented with 4 mmol/L of L-lactate (Wako Pure Chemical Industries) and 0.5% BSA. After purification, iPSC-CMs were replated and cultured in DMEM with 10% fetal bovine serum. All experiments were performed by ≈50 to 60 days of culture after the start of the differentiation.

CRISPR-Based Gene Correction Strategy

iPSC clones were generated with the same genetic background and precisely modified genotypes through homology-directed repair by using the CRISPR/Cas9 genome editing as described previously[32] (Expanded Methods and Materials; Table S2).

Introduction of Adeno-Associated Virus Vectors Into iPSC-CMs

Two days after replating, the medium was replaced with DMEM supplemented with 10% fetal bovine serum containing adenovirus vector–encoding human cMLCK or EGFP (enhanced green fluorescent protein) gene at a multiplicity of infection of 5.0×10^4. After 14 days of incubation, cells were fixed and immunostained with anti–α-actinin and anti-FLAG or recorded under electrical stimulation.

Mant-ATP Fluorescence Decay Curve Plot Assays and Analyses

Using a fluorescent ATP analog, Mant-ATP, chased with nonfluorescent ATP, we were able to deconvolute an abundance

of myosins in SRX and DRX conformations from the double-exponential fluorescent decay pattern. Mant-ATP assays were performed on the cardiac left ventricular (LV) tissues of mouse and human iPSC-CMs (day 56 differentiations) according to the protocol described previously.[33] LV tissues and monolayers of iPSC-CMs were incubated for 30 minutes (room temperature) in permeabilization buffer and flushed with glycerin before treatment with Mant-ATP. ZEISS LSM 880 with Airyscan was used with a "Plan-Apochromat" 20×/0.8 objective for fluorescence acquisition. In the experiments with purified cMLCK protein, the solutions contained 0.15 µmol/L of purified cMLCK. The fast decay in fluorescence intensity reflects myosins in DRX conformations, and slow decay reflects myosins in SRX conformations. Fluorescence emission was fitted to a biexponential decay equation.

LV Pressure-Volume Measurement

LV pressure-volume measurements using a Millar catheter were performed using the standard method[34] (Expanded Methods and Materials).

Cell Motion Imaging of Cultured Cardiomyocytes

In this study, we used the cell motion imaging system SI8000[35] for measuring the contractility of cultured cardiomyocytes because it can provide not only the contraction speed, but also the average deformation distance that is a surrogate marker for the force development of cultured cardiomyocytes[35] (Expanded Methods and Materials).

Kinase Activity Assay

Kinase activity assays were performed as described previously.[36] Kinase activities were assayed in 20 mmol/L of HEPES (pH 7.5), 1 mmol/L of $CaCl_2$, 5 mmol/L of $MgCl_2$, 2 mmol/L of dithiothreitol, 100 µmol/L of ATP, 0.01% of Tween 20, 100 nmol/L of calmodulin, with purified MLCKs and substrates in a 40-µL total volume at 25°C. Reaction mixtures were preincubated for 5 minutes, and the kinase reactions were started by the addition of ATP and incubated for the indicated time. For measurement of MLC K_m and V_{max} values, 5 nmol/L of cMLCK was incubated with 0.125 to 20 µmol/L of MLC2v at 25°C for 3 hours. Kinase activities were measured using ADP-Glo Kinase Assay[36] or Phos-tag SDS-PAGE[36] (Expanded Methods and Materials).

High-Throughput Screening for cMLCK Activators

8-Hydroxyquinoline structures were identified by high-throughput screening as an activator of cMLCK by the ADP-Glo and Kumagai method at 10 µmol/L, which posed >20% activation potency, whereas it did not exhibit any activation and inhibition of smooth muscle MLCK (smMLCK). Primary hit compounds were further optimized to have good potency as cMLCK activators and retained good permeability without cytotoxicity.

Statistics

All data are expressed as means±SD unless otherwise indicated. For 2-group comparisons, the 2-tailed Student *t* test was used. For multiple-group comparisons, 1-way ANOVA and Tukey correction were used. A *P* value <0.05 was considered statistically significant. Statistical analysis and graph generation were performed using GraphPad Prism (MDF; Tokyo, Japan).

Study Approval

All animal experiments were performed following the Guide for the Care and Use of Laboratory Animals (National Institutes of Health Publication, 8th Edition, 2011) and were approved by the Animal Care and Use Committee of the Osaka University Graduate School of Medicine. The genome research protocol was approved by the Human Genome Research Bioethical Committee at Osaka University. For the generation of iPSCs, written informed consent was obtained from patients before inclusion in the study according to the protocol approved by the institutional review board of Osaka University. Testing of human samples was approved by the ethics committee of Osaka University Hospital, and written informed consent was obtained from all patients before inclusion in the study.

RESULTS

KI Mice With Human DCM-Associated MYLK3 Mutant (c.1951-1G>T) Reproduced the Pathological Phenotype of DCM

We previously identified the DCM-associated, one single-nucleotide variant at the splice acceptor site of exon 9 in *MYLK3* (c.1951-1G>T; p.P639Vfs*15), which caused exon 9 skipping and frameshift and created a premature terminal codon.[21] To evaluate the functional sequence of this mutation in an animal model, we generated homozygous and heterozygous *Mylk3* mutation KI mice (*Mylk3*$^{fs/fs}$, *Mylk3*$^{+/fs}$) using CRISPR-Cas9–mediated homology-directed genome editing (Figure S1). Mice carrying the mutation were confirmed by PCR and Sanger sequencing (Figure 1A). Sequence analysis of the reverse transcription PCR product derived from mRNA showed that c.1951-1G>T mutation causes exon skipping and created a premature terminal codon (Figure 1A), similar to observations in humans.[21] To evaluate the levels of transcript expression from each allele, PCR probes that specifically detect wild-type and KI transcript were used (Figure S2). Droplet digital PCR analysis using cDNA from the hearts revealed that the copy number of the KI transcript was 90% lower than that of the wild-type transcript in heterozygous KI mice (Figure 1B), suggesting the instability of the transcripts from the KI allele due to a nonsense-mediated mRNA decay mechanism. The hearts from homozygous KI and heterozygous KI mice exhibited complete deficiency and a half-deficiency of cMLCK protein compared with those from wild-type mice, respectively (Figure 1C). The phosphorylation levels of MLC2v, a specific substrate of cMLCK, in the ventricles also decreased, depending on the level of cMLCK expression (Figure 1D). Cardiac pressure-volume loop analysis clearly demonstrated that homozygous KI mice showed

ORIGINAL RESEARCH ARTICLE

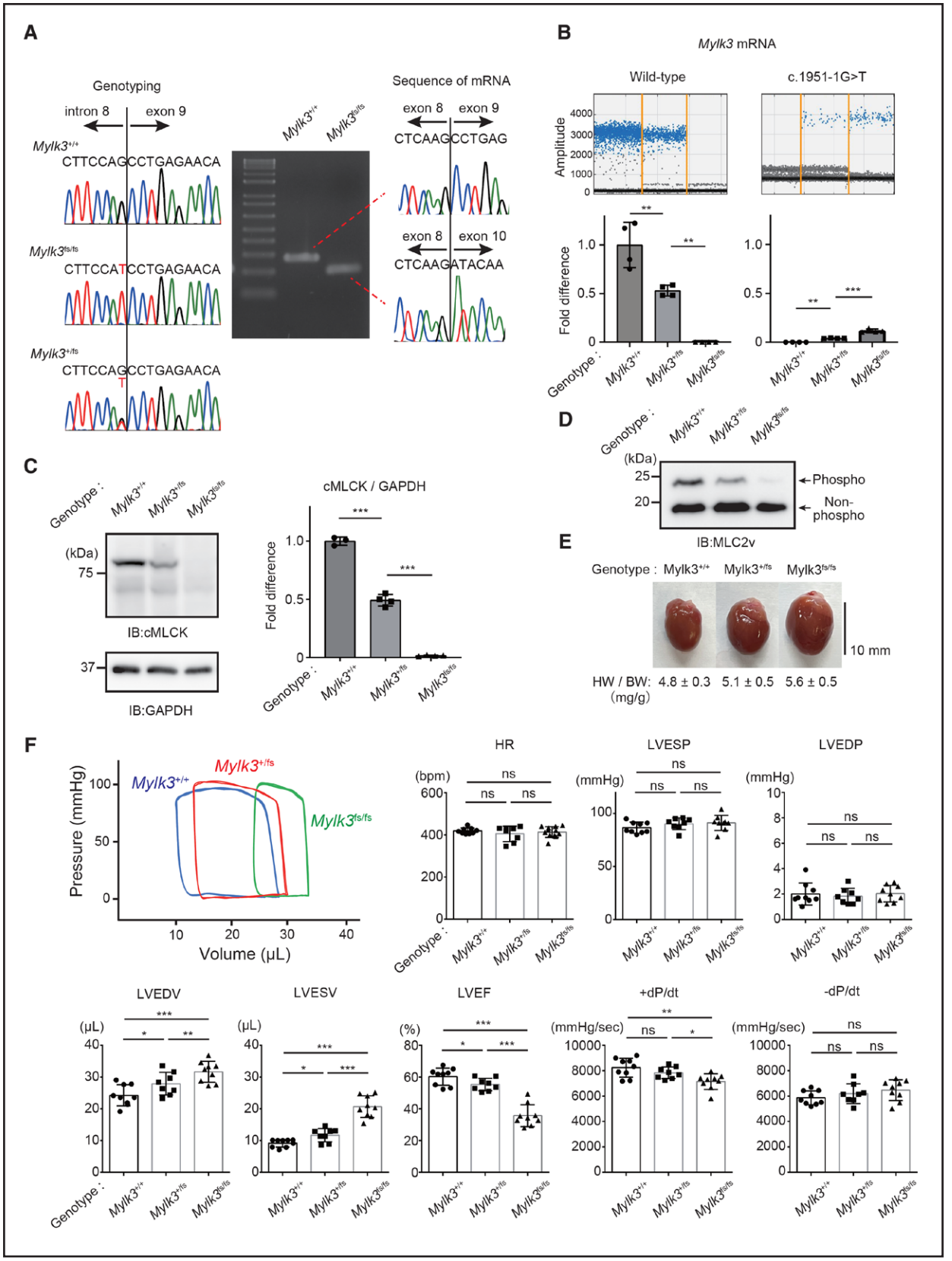

Figure 1. Knock-in mice with human dilated cardiomyopathy–associated *MYLK3* mutant (c.1951-1G>T) reproduced the phenotype of dilated cardiomyopathy.

A, Sanger sequencing analysis verified the presence of the c.1951-1G>T mutation at the splicing acceptor site of exon 9. Sequence analysis of the reverse transcription polymerase chain reaction products derived from mRNA of wild-type (MYLK3$^{+/+}$), heterozygous (*MYLK3*$^{+/fs}$), and homozygous (*MYLK3*$^{fs/fs}$) *Mylk3* mutant knock-in mice, showing out-frame skipping of exon 9 (71 bp) caused by the c1951-1 G>T (*Continued*)

Circulation. 2023;147:1902–1918. DOI: 10.1161/CIRCULATIONAHA.122.062885

Figure 1 Continued. mutation. **B**, Representative positive droplet signals from droplet digital polymerase chain reaction analysis. The concentration (copies/μL) of each transcript from the hearts of each mouse in the cDNA samples was normalized to that of the TBP (TATA-binding protein) transcript. Relative copy numbers were calculated as the ratio normalized to the value of the wild-type transcript (n=4 in each group). **C** and **D**, Whole-cell lysates were extracted from the ventricles of each mouse and analyzed using SDS-PAGE (**C**) or Phos-tag SDS-PAGE (**D**) followed by immunoblotting with the indicated antibodies. The ratio of cMLCK to GAPDH was calculated from the densitometry of immunoblots (n=3 to 4 in each group). Bands corresponding to phosphorylated and nonphosphorylated MLC2v were marked with open and closed circles, respectively. **E**, Representative images of the hearts were collected from 12-week-old MYLK3$^{+/+}$, *MYLK3*$^{+/fs}$, and *MYLK3*$^{fs/fs}$ mice. **F**, Representative tracing of the left ventricular pressure-volume curve of 12-week-old mice obtained by Millar micro-tip catheter examination and summarized data (n=8 to 12 in each group). Values are mean±SD (*P<0.05, **P<0.01, and ***P<0.001; 1-way ANOVA with Tukey post hoc test). cMLCK indicates cardiac-specific myosin regulatory light chain kinase; HR, heart rate; HW/BW, heart rate/body weight; IB, immunoblotting; LVEDP, left ventricular end-diastolic pressure; LVEDV, left ventricular end-diastolic volume; LVEF, left ventricular ejection fraction; LVESP, left ventricular end-systolic pressure; LVESV, left ventricular end-systolic volume; MLC2v, myosin regulatory light chain, ventricular/cardiac isoform; and ns, nonsignificant.

obvious LV dilatation with reduced LV contraction, whereas heterozygous KI mice showed LV dilatation with mildly reduced LV contraction compared with those of wild-type mice (Figure 1E and 1F; Figure S3). The hearts from homozygous KI mice showed slightly disrupted sarcomere structure without significant fibrosis (Figure S4). These results clearly demonstrated that the DCM-associated *MYLK3* mutation (c.1951-1G>T) resulted in depressed cMLCK activity and caused LV systolic dysfunction in vivo.

Restoration of cMLCK by AAV9-MYLK3 Vector Improved the Pathological Phenotypes of the Mylk3 Mutant (c.1951-1G>T) KI Mice

Next, we examined whether the upregulation of cMLCK could rescue the impaired LV contraction in vivo. Intravenous injection of the adeno-associated virus serotype 9 (AAV9) viral vectors carrying cardiac troponin T promoter and human *Mylk3* wild-type cDNA (AAV9-MYLK3 vector; 1.0×10^{11} vector genomes/ body; Figure 2A) into the retro-orbital venous sinus of 1-week-old mice achieved successful expression of the target genes preferentially in cardiomyocytes at 7 weeks after injection (Figure 2B and 2C). The transcript expression level of exogenous cMLCK by AAV9-MYLK3, detected by the specific probe for human *MYLK3*, was similar to that of endogenous *Mylk3*, detected by the specific probe for mouse *Mylk3*, in the wild-type hearts (Figure 2D; Figure S2). AAV-*MYLK3* vector improved LV dilatation and systolic function, whereas AAV9-*EGFP* vector did not improve them in homozygous KI mice (Figure 2E; Figure S5).

Upregulation of cMLCK Corrected the SRX/DRX Ratio in Cardiac Fibers From KI Mice With Mylk3 Mutation

To reveal the mechanistic insight, we next measured the abundance of myosin in SRX and DRX conformations in the skinned fibers from the mice using a fluorescent ATP analog, Mant-ATP. The cardiac fibers of the homozygous and heterozygous KI mice showed an increased abundance in SRX conformation compared with those of wild-type mice in proportion to the level of activity of cMLCK (Figure 3A). The treatment with purified cMLCK protein exogenously decreased the SRX conformation and increased the DRX conformations in the skinned cardiac fibers from KI mice (Figure 3B). We further examined the effect of AAV9-MYLK3 vector injection in the abundance of myosin in SRX and DRX. The cardiac fibers from the homozygous KI mice showed a decreased abundance in DRX conformation compared with those of wild-type mice, which was recovered to a similar level as in wild-type mice by AAV9-MYLK3 vector injection (Figure 3C). These results suggest that the downregulation of cMLCK in the myocardium causes LV systolic dysfunction by increasing the SRX/DRX ratio, which could be corrected by cMLCK upregulation.

iPSC-CMs From the Carrier of c.1951-1G>T Variant (MYLK3$^{+/fs}$) Showed Decreased MLC2v Phosphorylation Levels With Reduced Contractility

To examine whether the cardiac dysfunction observed in the KI mice was reproduced in human cardiomyocytes, we established iPSC from the carrier of heterozygous c.1951-1G>T variant (*MYLK3*$^{+/fs}$; Figure 4A) and differentiated the iPSC into cardiomyocytes (iPSC-CMs). Sequence analysis of the reverse transcription PCR product derived from mRNA showed that c.1951-1G>T mutation causes exon skipping and created a premature terminal codon (Figure S6). To evaluate the levels of transcript expression from wild-type alleles in iPSC-CMs, a droplet digital PCR probe that specifically detects wild-type human *MYLK3* transcript was used (Figure S7). Analysis of mRNA transcripts revealed that *MYLK3*$^{+/fs}$ iPSC-CMs have a 2-fold lower expression level of wild-type *MYLK3* mRNA than the control wild-type iPSC-CMs (MYLK3$^{+/+}$; Figure 4B). The cMLCK protein and MLC2v phosphorylation levels in *MYLK3*$^{+/fs}$ iPSC-CMs were also much lower than those in MYLK3$^{+/+}$ iPSC-CMs (Figure 4C and 4D). Consistent with these data, *MYLK3*$^{+/fs}$ iPSC-CMs showed reduced contractility compared with MYLK3$^{+/+}$ iPSC-CMs (Figure 4E). CRISPR-mediated gene-corrected *MYLK3*$^{+/fs}$ iPSC (c.1951-1T>G corrected; Figure 4A) completely recovered the mRNA (Figure 4B) and protein expression levels (Figure 4C) of wild-type *MYLK3*, MLC2v phosphorylation level (Figure 4D), and contractility (Figure 4E) to

ORIGINAL RESEARCH ARTICLE

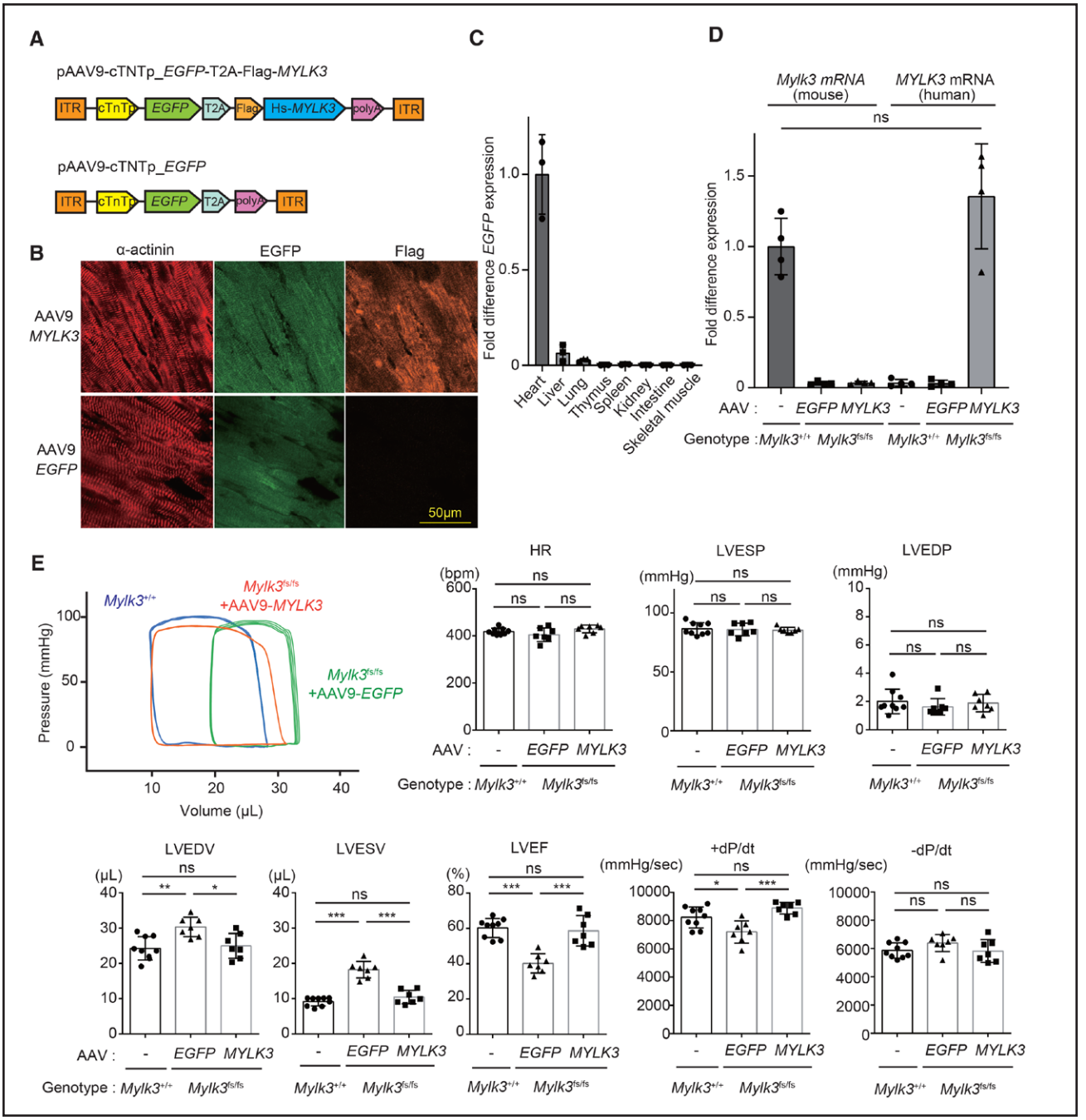

Figure 2. The phenotype of *Mylk3* mutant (c.1951-1G>T) knock-in mice was rescued by AAV9-cMLCK.
A, Schematic representations of the AAV9-MYLK3 vector encoding for EGFP and human MYLK3 cDNA and the EGFP control vector. **B** and **C**, Immunohistochemical staining and quantitative polymerase chain reaction analysis showed that AAV9 application through the retro-orbital sinus in 1-week-old mice resulted in efficient cardiac expression of the target genes. **B**, Immunohistochemical staining for α-actinin, EGFP, and Flag on the left ventricles from homozygous knock-in mice at 4 weeks after AAV vector injection (bar=50 μm). **C**, Quantitative polymerase chain reaction analysis of *EGFP* mRNA expression level in various tissues of knock-in mice at 8 weeks after AAV vector injection. *EGFP* mRNA levels were normalized to those of *Gapdh*, and the average of the *EGFP*/*Gapdh* in the heart was defined as 1 (n=3 in each tissue). **D**, The concentration (copies/μL) of each transcript in the hearts were measured by droplet digital polymerase chain reaction using specific probe and primers (Figure S2B), which were normalized to that of the TBP (TATA-binding protein) transcript. Relative copy numbers were calculated as the ratio normalized to the value of the wild-type mouse *Mylk3* transcript (n=4 in each group). **E**, Representative tracing of left ventricular pressure-volume curve of the homozygous knock-in mice at 11 weeks after AAV injection obtained by Millar micro-tip catheter examination and summarized data (n=7 to 9 in each group). Values are mean±SD (*P<0.05 and **P<0.01; 1-way ANOVA with Tukey post hoc test). AAV indicates adeno-associated virus; cTnT, chicken cardiac troponin promotor; EGFP, enhanced green fluorescent protein; HR, heart rate; ITR, inverted terminal repeat; LVEDP, left ventricular end-diastolic pressure; LVEDV, left ventricular end-diastolic volume; LVEF, left ventricular ejection fraction; LVESP, left ventricular end-systolic pressure; LVESV, left ventricular end-systolic volume; ns, nonsignificant; polyA, rabbit globin polyA tail; and T2A, a sequence of T2A self-cleaving peptide.

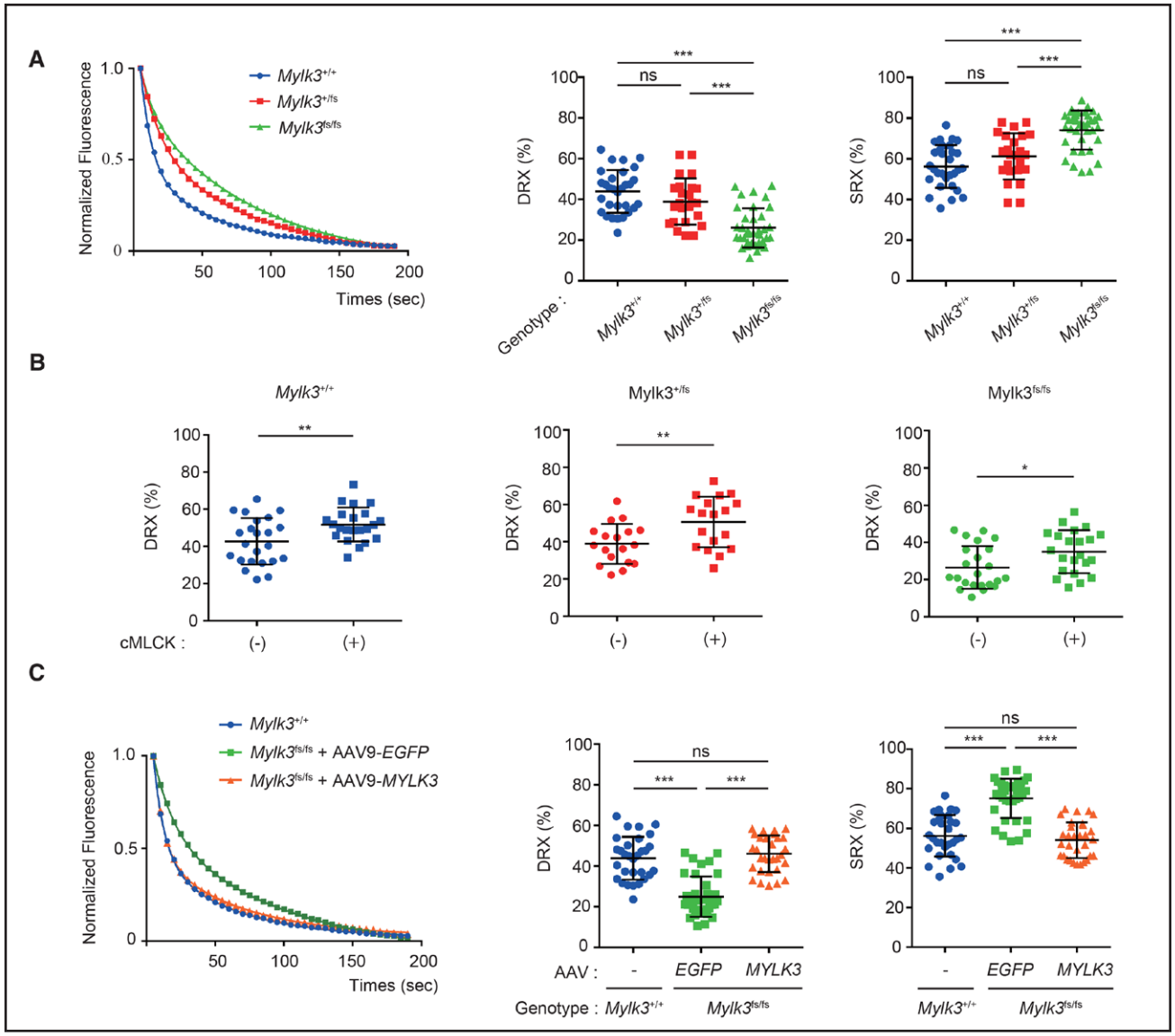

Figure 3. Upregulation of cMLCK corrected the SRX/DRX ratio in cardiac fibers from KI mice with *Mylk3* mutation.
A, Representative Mant-ATP fluorescence decay curves plot of myocardium from each mouse and proportions of myosin heads in the DRX conformation and SRX conformation. Data were obtained from studies of 3 hearts in each mouse, with 4 to 5 samples studied per heart. **B**, Proportions of myosin heads in the DRX conformation in myocardium from each mouse before and after the treatment with purified cMLCK, which were determined by Mant-ATP assay. Data were obtained from studies of 3 hearts in each mouse, with 4 to 5 samples studied per heart. **C**, Representative Mant-ATP fluorescence decay curve plot of myocardium from each mouse with the indicated treatment and proportions of myosin heads in the DRX conformation and the SRX conformation. Data were obtained from studies of 3 hearts in each mouse, with 4 to 5 samples studied per heart. Values are mean±SD (*P<0.05, **P<0.01, and ***P<0.001; 1-way ANOVA with Tukey post hoc test [**A** and **C**] or Student t test [**B**]). AAV indicates adeno-associated virus; cMLCK, cardiac-specific myosin regulatory light chain kinase; DRX, disordered relaxed state conformation of myosin molecule; ns, nonsignificant; and SRX, super-relaxed state conformation of the myosin molecule.

the same degree as MYLK3$^{+/+}$ iPSC-CMs. These results indicate that downregulation of cMLCK can cause decreased contractility in human cardiomyocytes also.

Restoration of cMLCK by AAV9-MYLK3 Vector Improved the Pathological Phenotypes of the Human MYLK3$^{+/fs}$ iPSC-CMs

Next, we examined whether the upregulation of cMLCK could rescue the reduced contractility by modulating the ratio of SRX/DRX conformations. *MYLK3*$^{+/fs}$ iPSC-CMs were transduced with AAV9-MYLK3 vector by adjusting to obtain similar expression levels of mRNA (Figure 5A) and protein (Figure 5B) of wild-type *MYLK3* in MYLK3$^{+/+}$ iPSC-CMs, which recovered MLC2v phosphorylation level (Figure 5C) and contractility (Figure 5D), accompanied by the decreased ratio of SRX/DRX (Figure 5E). These results suggest that upregulation of cMLCK can enhance contractility in human cardiomyocytes. Therefore, we hypothesized that chemical compounds that activate

ORIGINAL RESEARCH ARTICLE

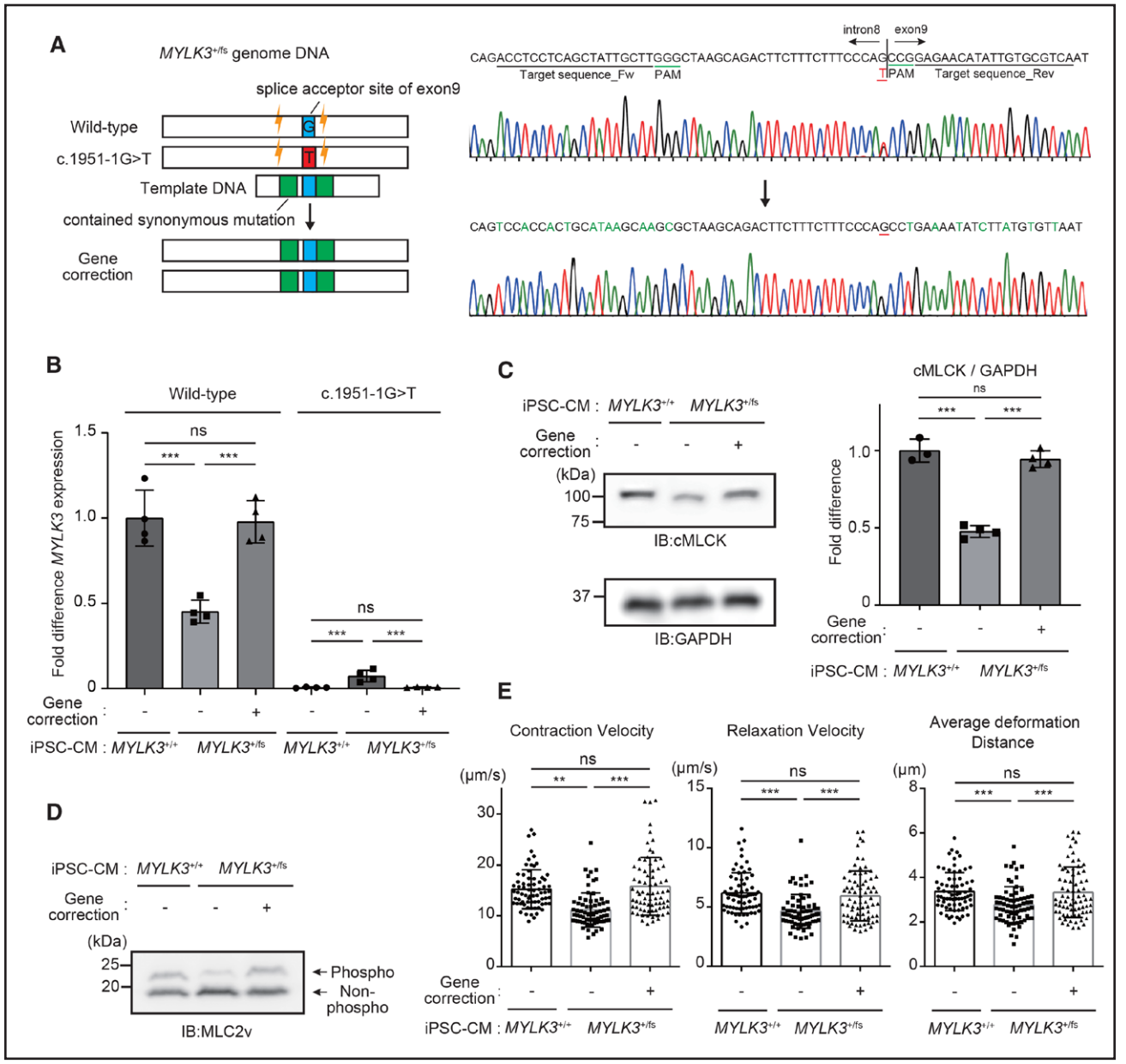

Figure 4. Human iPSC-CMs from the carrier of c.1951-1G>T mutant showed decreased MLC2v phosphorylation level with reduced contractility.

A, Scheme for gene editing for gene correction of iPSCs with heterozygous c.1951-1G>T mutant in *MYLK3*. For the CRISPR gene correction strategy, single-guide RNAs were designed. Single-stranded oligodeoxynucleotides used for genomic repair contained the wild-type sequence at the mutation site (blue), and synonymous mutations (green), as well, to remove the PAM site to prevent recutting of the corrected allele while preserving the amino acid sequence. **B**, mRNA expression levels of wild-type and c.1951-1G>T mutant *MYLK3* were measured using droplet digital polymerase chain reaction analysis in wild-type, *MYLK3*$^{+/fs}$, or gene-corrected iPSC-CMs. The concentrations (copies/μL) of each transcript were normalized to those of *TBP*. Relative copy numbers were calculated as the ratio normalized to the value of the wild-type *MYLK3* in wild-type iPSC-CMs (n=4 in each tissue). **C** and **D**, Whole-cell lysates from iPSC-CMs were analyzed using SDS-PAGE (**C**) or Phos-tag SDS-PAGE (**D**) followed by immunoblotting with the indicated antibodies. The ratio of cMLCK to GAPDH was calculated from the densitometry of immunoblots (n=3 to 4 in each tissue). **E**, Maximum contraction velocity, maximum relaxation velocity, and average deformation distance in the monolayer of iPSC-CMs on day 56 after the differentiation were calculated using motion vector analysis. The number of analyzed regions of interest were 70, 70, and 75 for MYLK3$^{+/+}$, *MYLK3*$^{+/fs}$, and the gene-corrected (*MYLK3*$^{+/+}$) iPSC-CMs, respectively. Data were collected from 3 independent experiments. Values are mean±SD (*P<0.05, **P<0.01, and ***P<0.001; 1-way ANOVA with Tukey post hoc test). cMLCK indicates cardiac-specific myosin regulatory light chain kinase; IB, immunoblotting; iPSC-CM, induced pluripotent stem cell–derived cardiomyocyte; MLC2v, myosin regulatory light chain, ventricular/cardiac isoform; and ns, nonsignificant.

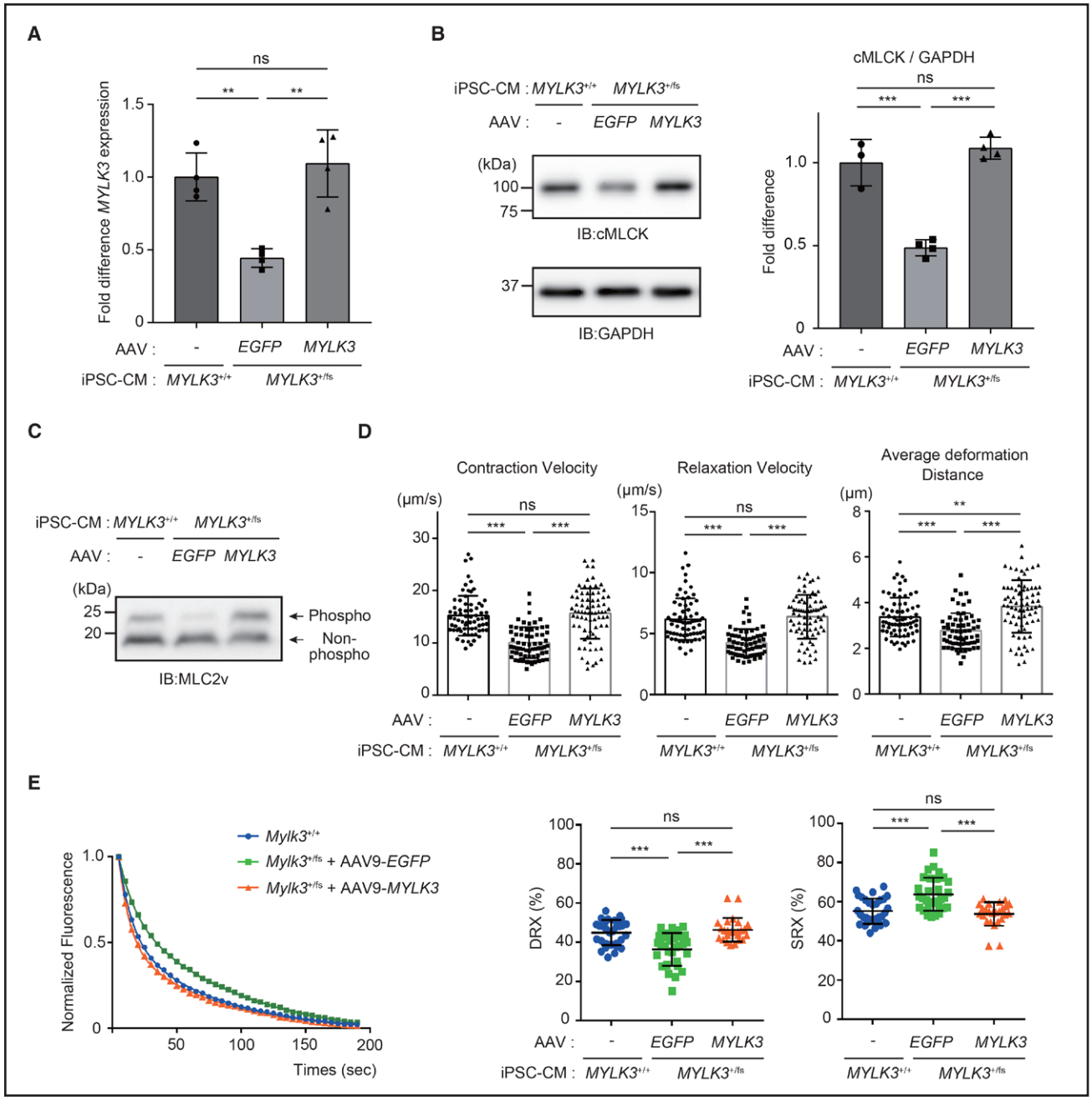

Figure 5. The phenotype of *MYLK3*$^{+/fs}$ iPSC-CMs was rescued by AAV9-MYLK3.

A, The concentrations (copies/μL) of wild-type human *MYLK3* transcript were measured by droplet digital polymerase chain reaction using specific probe and primers (Figure s2B) in *MYLK3*$^{+/fs}$ human iPSC-CMs treated with AAV9-*MYLK3*. *MYLK3* transcription levels were normalized to that of the TBP (TATA-binding protein) transcript. Relative copy numbers were calculated as the ratio normalized to the value of the wild-type iPSC-CMs n=4 in each tissue). **B** and **C**, Whole-cell lysates from human iPSC-CMs were analyzed using SDS-PAGE (**C**) or Phos-tag SDS-PAGE (**D**) followed by immunoblotting with the indicated antibodies. The ratio of cMLCK to GAPDH was calculated from the densitometry of immunoblots (n=3 to 4 in each tissue). Bands corresponding to phosphorylated and nonphosphorylated MLC2v were marked with open and closed circles, respectively. **D**, Maximum contraction velocity, maximum relaxation velocity, and average deformation distance in the monolayer of iPSC-CMs on day 56 after the differentiation were calculated using motion vector analysis. The number of analyzed regions of interest were 70, 65, and 75 for *MYLK3*$^{+/+}$ iPSC-CMs, *MYLK3*$^{+/fs}$ treated with AAV9-*EGFP*, and *MYLK3*$^{+/fs}$ treated with AAV9-*MYLK3*, respectively. Data were collected from 3 independent experiments. **E**, Representative Mant-ATP fluorescence decay curve plots and the proportions of myosin heads in the DRX conformation and in SRX conformation in human iPSC-CM with the indicated treatments (n=25 to 31 in each). Values are mean±SD (*P<0.05, **P<0.01, and ***P<0.001; 1-way ANOVA with Tukey post hoc test). AAV indicates adeno-associated virus; cMLCK, cardiac-specific myosin regulatory light chain kinase; DRX, disordered relaxed state conformation of myosin molecule; IB, immunoblotting; iPSC-CM, induced pluripotent stem cell–derived cardiomyocyte; MLC2v, myosin regulatory light chain, ventricular/cardiac isoform; ns, nonsignificant; and SRX, super-relaxed state conformation of the myosin molecule.

endogenous cMLCK could also enhance contractility in cardiomyocytes.

cMLCK Activator Improved the Pathological Phenotypes of the Human MYLK3$^{+/fs}$ iPSC-CMs

Enhancement of the cardiac sarcomere contractility can be achieved conceptually by upregulation of MLC2v phosphorylation by the activation of cMLCK, without changes in cardiomyocyte calcium homeostasis. Therefore, we performed a high-throughput screening (using the ADP-Glo assay at a concentration of 10 µmol/L). The primary hit compound was further optimized to afford the cMLCK activator LEUO-1154 (Figure 6A; Figure S8). LEUO-1154 showed good potency and concentration-dependent activation of cMLCK with a half-maximal effective concentration value of 2.30 µmol/L, with a 95% CI of 1.64 to 3.22 µmol/L (Figure 7B). LEUO-1154 had little or no effect on skeletal muscle MLCK (skMLCK) and smMLCK (Figure 6B), showing its selective activation for cMLCK. LEUO-1154 induced an ≈2-fold increase in the apparent V_{max} for MLC2v phosphorylation of cMLCK without affecting the apparent K_m for MLC2v (Figure 6C), indicating that LEUO-1154 activates cMLCK allosterically. Next, we examined the effect of LEUO-1154 using the human iPSC-CMs. LEUO-1154 significantly increased the contraction velocity and averaged deformation distance (Figure 6D) without affecting the calcium transients (Figure S9A) in *MYLK3*$^{+/fs}$ iPSC-CMs at 56 days after differentiation. This was accompanied by the upregulated MLC2v phosphorylation level (Figure S9B) and increased the SRX/DRX ratio (Figure 6E) to the same degree as *MYLK3*$^{+/+}$ iPSC-CM. Moreover, we evaluated the effects of LEUO-1154 on the contractile force using 3-dimensional self-organized tissue rings.[37,38] The maximum force in self-organized tissue rings from the *MYLK3*$^{+/fs}$ iPSC-CMs significantly increased after treatment with LEUO-1154 (Figure 6F). These results suggest that the allosteric activation of cMLCK by small-molecule compounds can enhance the contractility in human cardiomyocytes with myosin regulatory light chain phosphatase dominancy. Furthermore, we examined the effects of the compound on different models of DCM, human iPSC-CMs with homozygous stop-gain mutations in the desmoglein-2 (*DSG2*) gene (*DSG2*-R119X iPSC-CMs) reported previously.[38] LEUO-1154 significantly increased the contraction velocity and averaged deformation distance (Figure S10) in *DSG2*-R119X iPSC-CMs and increased the maximum force in self-organized tissue rings from *DSG2*-R119X iPSC-CMs (Figure 6G).

Human Failing Hearts Showed a Reduced Ratio of MYLK3/PPP1R12B

The phosphorylation level of a protein is given by a balance between the activity of protein kinase and protein phosphatases. The extent of MLC2v phosphorylation is primarily determined by the balance between cMLCK and myosin regulatory light chain phosphatase[24,29] (Figure S11). In cardiac muscle, the major functional subunit of myosin regulatory light chain phosphatase is myosin phosphatase targeting protein 2 (MYPT2), encoded by the *PPP1R12B* gene, and the overexpression of MYPT2 in the heart decreases MLC2v phosphorylation.[39] Therefore, we examined the balance between cMLCK and MYPT2 in the failing myocardium of patients with advanced HF (Figure S12) by measuring mRNA expressions of *MYLK3* and *PPP1R12B* by digital droplet PCR. All cardiac tissues from the patients demonstrated decreased expression levels of *Mylk3* mRNA compared with those from human control cardiac tissue (Figure 7A), and the ratios of *MYLK3/ PPP1R12B* mRNA were markedly decreased in all the failing hearts (Figure 7B). These results indicate the dominance of myosin regulatory light chain phosphatase over cMLCK even in failing human hearts without *MYLK3* mutations.

DISCUSSION

MYLK3 Mutation Reproduced Systolic Dysfunction in Mice Models and iPSC-CMs

The 3 mutations in *MYLK3* that have been identified in humans so far are associated with human DCM pathogenesis: a read-through mutation (c.2459A>C; p.820Sext*19),[40] a frameshift mutation (c.1879_1885del; p.L627fs*41),[40] and a frameshift mutation (c.1951-1G>T; p.P639Vfs*15).[21] Here, we generated KI mice with the c.1951-1G>T mutation, which revealed a decreased level of the transcript from the mutant allele compared with the wild-type allele, suggesting that the c.1951-1G>T mutation leads to nonsense-mediated mRNA decay. The expressions of wild-type *MYLK3* mRNA and cMLCK protein in the hearts from the heterozygous or homozygous KI mice came down by half compared with those from wild-type mice or could not be detected, respectively. Depending on the expression level of cMLCK, the KI mice showed marked reductions in MLC2v phosphorylation and developed systolic HF. *MYLK3*$^{+/fs}$ iPSC-CMs also showed reduced contractility, although *Mylk3*$^{+/fs}$ mice, in which MLC2v phosphorylation was decreased by 50%, showed only mild LV dilatation without obvious LV systolic dysfunction. The relationship between MLC2v phosphorylation level and the ability of a cardiac muscle to produce force and power were clearly demonstrated previously, using the LV traveculae.[11] It is noteworthy that decreasing MLC2v phosphorylation causes a more prominent effect on force production because decreasing MLC2v phosphorylation by only 30% from the in vivo control level, reduced force generation by a remarkable 75%, whereas increasing MLC2v phosphorylation by 50% increased force generation by only

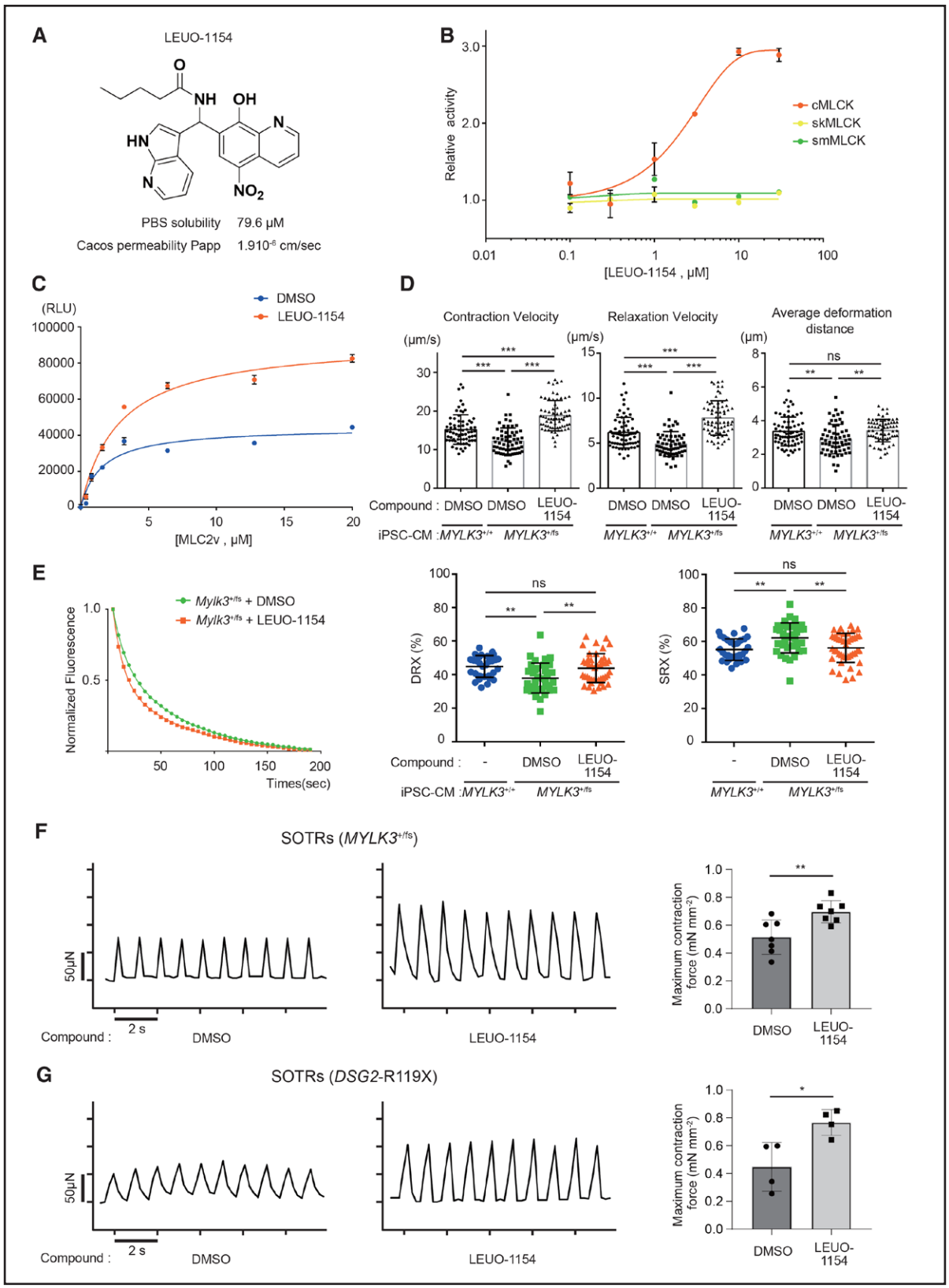

Figure 6. cMLCK activator improved contraction and relaxation in human *MYLK3*$^{+/fs}$ iPSC-CMs.
A, The chemical structure of LEUO-1154, a cMLCK activator. **B**, The dose-response effects of LEUO-1154 on the activities of human cMLCK, skMLCK, and smMLCK were determined by in vitro kinase assay using ADP-Glo (n=3 for each point) **C**, MLC2v dose dependence of human cMLCK activities in the presence of LEUO-1154. The reactions that contained no MLC2v were set as a background. The luminescence readings of the reactions were corrected with background subtraction and finally fit with the Michaelis-Menten equation. K_m(MLC2v) values (*Continued*)

Figure 6 Continued. of human cMLCK were 1.57±0.58 or 2.81±0.53 μmol/L, and maximum luminescence values were 44 400±4400 or 92 800±5500 relative light unit (RLU) that corresponded to a V_{max} of 3.31±0.19 or 7.10±0.27 mol·min^{-1}·mol^{-1} kinase in the presence of DMSO or LEUO-1154 (10 μmol/L), respectively (n=3 for each point). **D**, Effect of LEU-1154 (10 μmol/L for 3 days) on cardiac contraction and relaxation in *MYLK3*$^{+/fs}$ iPSC-CMs. n61 or 69 for DMSO or LEUO-1154, respectively. **E**, The effect of LEU-1154 (10 μmol/L) on the proportions of myosin heads in the DRX and in SRX conformations in *MYLK3*$^{+/fs}$ iPSC-CM analyzed by the Mant-ATP assay (n=31 to 43 in each). **F** and **G**, The effect of LEU-1154 (10 μmol/L) on SOTRs generated from either *MYLK3*$^{fs/+}$ iPSC-CMs (**F**) or *DSG2*-R119X iPSC-CMs (**G**). Representative micro-force traces and the calculated average maximum forces were shown (n=4 to 7 in each). cMLCK indicates cardiac-specific myosin regulatory light chain kinase; DMSO, dimethyl sulfoxide; DRX, disordered relaxed state conformation of myosin molecule; IB, immunoblotting; iPSC-CM, induced pluripotent stem cell–derived cardiomyocyte; MLC2v, myosin regulatory light chain, ventricular/cardiac isoform; ns, nonsignificant; skMLCK, skeletal muscle type myosin regulatory light chain kinase; smMLCK, smooth muscle type myosin regulatory light chain kinase; SOTRs, self-organized tissue rings; and SRX, super-relaxed state conformation of the myosin molecule.

24%.[11] Therefore, the reduction of MLC2v phosphorylation by 50% observed in *MYLK3*$^{+/fs}$ iPSC-CMs is enough to be considered as a cause of reduced contractility. The *Mylk3*$^{+/fs}$ developed LV dilatation with mildly reduced LV contraction. Thus, this is the first report to demonstrate that the *MYLK3* mutation associated with human DCM faithfully reproduced the DCM phenotypes in vivo. Our results are consistent with the phenotypes of *Mylk3* knockout mice,[18] strongly supporting the idea that reduced activity of cMLCK causes DCM in humans.

Upregulation of cMLCK Rescued Systolic Dysfunction by Decreasing the SRX/DRX Ratio

To our knowledge, this is the first study to demonstrate that cMLCK activity regulates cardiac contractility by changing the SRX/DRX ratio in mammalian cardiomyocytes. Restoration of cMLCK expression in the heart of *Mylk3*$^{fs/fs}$ by AAV9-*MYLK3* vector successfully recovered the DCM phenotype. Cardiac myofibers from the *Mylk3*$^{fs/fs}$ mice had decreased the SRX/DRX ratio compared with those from *Mylk3*$^{+/+}$ mice, whereas the myofibers from *Mylk3*$^{fs/fs}$ mice treated with AAV-*MYLK3* vector had an SRX/DRX ratio comparable to that from *Mylk3*$^{+/+}$. SRX is a well-ordered structure of myosin in which paired myosin heads interact through an interacting-heads motif and dock onto the thick filament backbone, which inhibits its myosin ATPase activity and withdraws both myosins from thin filament interaction and force production.[26,41] MLC2 phosphorylation by cMLCK reduces myosin SRX by disrupting interacting-heads motif interactions and increases the abundance of cross-bridges in proximity to the thin filament, DRX state in cardiac muscle.[12,41–43] In addition, MLC2v phosphorylation accelerates the rate of force redevelopment after muscle release[11] and increases the force of individual cross-bridges.[7,44] Thus, cMLCK activation is proposed to increase the ensemble force produced in striated muscles[8,27] by increasing the constant *Nt* (the total number of cross-bridges that are functionally accessible for interaction with actin thin filaments) and $f_{intrinsic}$ (the intrinsic force of a single myosin motor). The present study demonstrated the positive effects of cMLCK on both the contraction velocity and the average deformation distance, a surrogate marker for the force development of cultured cardiomyocytes.[35] Thus, cMLCK reactivation can increase the power (force × velocity) of the contraction and represents the ability of the heart to pump blood efficiently.[8]

cMLCK Is a Potential Target for Advanced HFrEF

In the clinical situations of reduced myocardial contractile function, such as HFrEF, including DCM and old myocardial infarction, targeting MLC2v phosphorylation may have a beneficial effect on salvaging systolic insufficiency through 2 distinct mechanisms: enhancement of the contraction and rearrangement of sarcomere structure. In the present study, we demonstrated the dominant mRNA expression of myosin light chain phosphatase over cMLCK in human failing myocardium, which is consistent with previous reports showing increased cardiac phosphatase[45] and decreased MLC2v phosphorylation[22,46] in end-stage failing human hearts. Many studies using animal models of HF support these findings. Overexpression of MYPT2 in the heart caused decreased MLC2v phosphorylation by accumulating the catalytic subunit PP1cδ bound to excess MYPT2.[39] Pressure overload by transverse aortic constriction surgery in mice reduced cMLCK expression by 85% and the extent of MLC2v phosphorylation by 40%.[19] The conditional knockdown of cMLCK protein in mice caused depressed cardiac performance when MLC2v phosphorylation was reduced.[20] A myocardial infarction model also showed decreased phosphorylation level of MLC2v depending on the time course and severity of the diseases.[19,47–49] Because cMLCK also plays key roles in the adaptive responses to physical[50] and pathophysiological stresses,[18] reduced expression or activity of cMLCK may contribute to the transition from compensated to decompensated cardiac hypertrophy in pathological situations.[19] On the other hand, upregulated MLC2v phosphorylation contributed to twice as much power production of compensated myocardium taken at distant sites from the infarct zone compared with the noninfarcted control in a chronic rat myocardial infarction model.[51] Overexpression of cMLCK in cardiomyocytes also protected the heart against cardiac dysfunction during pressure overload.[19] We also demonstrated a beneficial effect of cMLCK activation using self-organized tissue rings from iPSCs derived from a

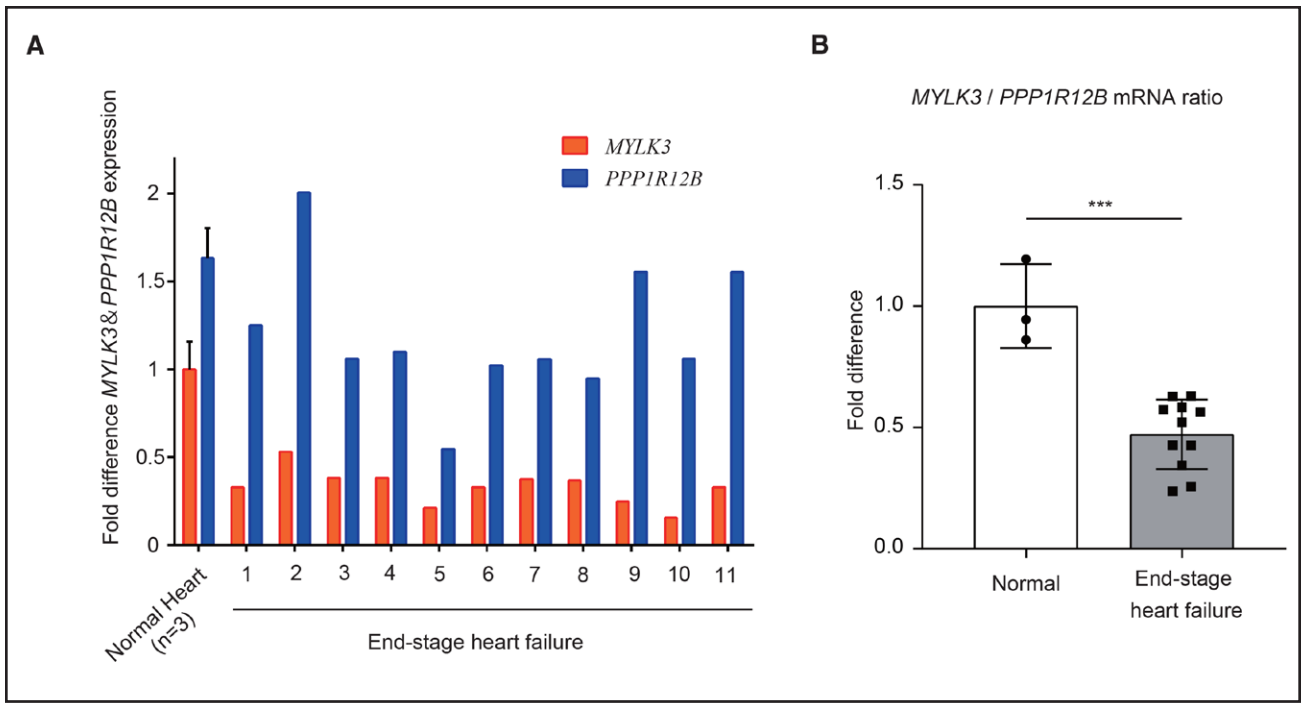

Figure 7. Human failing hearts showed a reduced ratio of cMLCK/MYPT2.
A, The concentrations (copies/μL) of *MYLK3* and *PPP1R12B* transcript in left ventricular tissues from the control or patients with end-stage heart failure were measured by droplet digital polymerase chain reaction analysis, which was normalized to that of the TBP (TATA-binding protein) transcript. The relative copy number was calculated as the ratio normalized to the value of the transcript in normal hearts (n=4). **B**, The ratio of *MYLK3*/*PPP1R12B* transcripts in left ventricular tissues was calculated from the data of **A**. Values are mean±SD (***P<0.001; 1-way ANOVA with Tukey post hoc test).

patient who had DCM with mutations other than those in *MYLK3* in this study. We suggest that restoration of cMLCK function can improve contractility in conditions whereby contractile dysfunction is not caused by *MYLK3* mutations. In addition, previous reports have shown that MLC2v phosphorylation by cMLCK promotes sarcomere assembly and organization in vertebrate cardiac muscle.[13–15] Sarcomere disorganization is a well-documented characteristic of cardiomyocytes in the failing myocardium of human and animal models.[51] Therefore, reactivation of cMLCK may promote sarcomere reorganization in failing myocardium, which improves cardiac function from the viewpoint of cardiac sarcomere structure.

Development of Allosteric cMLCK Activators and Comparison With OM and Other Inotropes

cMLCK expresses exclusively in cardiomyocytes and has a specificity for MLC2 as a substrate.[15] These main features of cMLCK make this enzyme an attractive target for therapeutic intervention in HFrEF. cMLCK belongs to the $Ca2^{+}$/calmodulin-activated protein kinase family.[52] It contains a conserved kinase domain and a regulatory domain (autoinhibitory domain and calmodulin-binding domain) at its C terminus, with 58% identity with skMLCK and 44% identity with smMLCK.[16] On the other hand, the N terminus of cMLCK lacks homologies to known proteins including other MLCK family proteins. Performing high-throughput screening and synthesizing the lead structure and numerous analogues allowed us to identify allosteric cMLCK-specific activators. These agents were found to be selective for cMLCK versus smMLCK and skMLCK isoforms and demonstrated improved contractility without affecting the intracellular calcium dynamics in human iPSC-CMs.

OM has recently provided a clinically meaningful reduction in the composite end point of the time to first HF event and cardiovascular death among patients with severe HFrEF.[1,3,53] OM, a first-in-class small-molecule activator of cardiac myosin II,[4,5] is classified as a myotrope that can improve cardiac contractility through directly activating sarcomere proteins without affecting intracellular calcium dynamics.[2,5] Therefore, myotropes are expected to provide a new therapeutic approach for severe HFrEF, as they can improve hemodynamic status without the adverse clinical events associated with increased intracellular calcium concentration that is observed with traditional inotropes.[2,5] The cMLCK activators described here can also be classified as myotropes and a first-in-class small molecule activator of cMLCK. In contrast with OM that enhances the ensemble force ($F_{ensemble}$) produced from sarcomere mainly by increasing

the duty ratio (the fraction of accessible myosin heads strongly bound to actin at any point during contraction),[4] cMLCK activator enhances $F_{ensemble}$ probably by increasing both Nt^{43} and $f_{intrinsic}$[7] through MLC2v phosphorylation. Thus, OM and cMLCK activators can enhance sarcomere contraction by different mechanisms, which broadens treatment options and could provide an additive or synergistic beneficial effect on the cardiac performance in patients with severe HFrEF.

Our cMLCK activator has one notable limitation. It can activate only human cMLCK and cannot activate cMLCK from other species, probably because the N terminus of cMLCK lacks homologies between species (Figure S13). Our cMLCK activator cannot activate the N-terminus deletion mutant of human cMLCK or the cMLCK from other species, such as rats and mice (Figure S14). Therefore, the present study lacks application to animal experiments, and we could not demonstrate the effects of the cMLCK activator in vivo. However, considering the prominent reduction of force generation by decreasing MLC2v phosphorylation,[11] it is conceivable that the correction of MLC2v phosphorylation level has the potential to improve cardiac contractility in failing myocardium where the MLC2v phosphorylation level is decreased.

In conclusion, reduced cMLCK activity contributes to the development and progression of advanced HF in humans, and the recovery of cMLCK activity could be an attractive approach for the treatment of cardiac contractile dysfunction. Allosteric cMLCK activators have the potential to be a new class of myotrope for the treatment of HFrEF.

ARTICLE INFORMATION

Received October 16, 2022; accepted April 5, 2023.

Affiliations

Department of Medical Biochemistry, Osaka University Graduate School of Medicine/Frontier Biosciences, Suita, Osaka, Japan (T.H., O.T., K.M., H. Kioka, H. Kato, H.H., Y.S., C.O., H.I., J.H., K.U., T.S., S.N., S.T.). Department of Cardiology (Y.K., S.H., S.O., H. Kioka, HY.H., S.N., Y.A., Y.S.), Department of Cardiovascular Surgery (J.L., L.L.), Osaka University Graduate School of Medicine. Suita, Osaka, Japan. Department of Cardiovascular Medicine, Graduate School of Medical Science, Kanazawa University. Kanazawa, Ishikawa, Japan (N.F., S.Y., M.T.). Department of Genomic Medicine, National Cerebral and Cardiovascular Center, Osaka, Japan (Y.A.). Department of Internal Medicine, Meiji University of Integrative Medicine, Nantan, Kyoto, Japan (H.A.). Compound Library Screening Center (A.T.), Lead Explorating Units (S.K., T.K., J.-i.H.), Graduate School of Pharmaceutical Sciences, Osaka University, Suita, Osaka, Japan. Drug Discovery Initiative, Graduate School of Pharmaceutical Sciences, The University of Tokyo, Bunkyo-ku, Tokyo, Japan (R.I.). Hanwa Memorial Hospital, Sumiyoshi-ku, Osaka, Japan (M.K.).

Acknowledgments

Drs Hitsumoto and Tsukamoto primarily performed the experiments and analyzed the data. Drs Li, Liu, Kuramoto, Higo, Ogawa, and Hitsumoto generated iPS cells and CRISPR-Cas gene editing. Drs Fujino, Yoshida, Kioka, Asano, Takamura, and Saito acquired and analyzed clinical data. Drs Matsuoka and Kuramoto contributed to genome informatics analysis. Drs Tsukamoto, Matsuoka, and Hitsumoto contributed to the generation of KI mice. Drs Tsukamoto, Saito, Tani, and Imamura performed the high-throughput screening assay for cMLCK activators. Drs Komagawa, Kanai, and Haruta were responsible for the design and preparation of the cMLCK activator, LEUO-1154. Drs Matsuoka, Hakui, Okamoto, Inouse, Hyejin, Ueda, Segawa, Nishimura, Asanuma, Kitakaze, and Takashima analyzed the data and revised the manuscript. Drs Tsukamoto and Takashima were responsible for the overall direction of the project and interpretation of the data. Drs Tsukamotot and Hitsumoto wrote the article. The authors thank the patient and his family members for their contribution to this study. We thank Editage (www.editage.com) for English language editing.

Sources of Funding

This work was supported by grants-in-aid from the Japan Agency for Medical Research and Development (AMED [JP19nk0101341 and 21bm0804008h0005]), by Platform Project for Supporting Drug Discovery and Life Science Research (Basis for Supporting Innovative Drug Discovery and Life Science Research [BINDS]) from AMED (under JP21am0101084 and JP21am0101085 [support numbers 1745, 2464, 2677, 2678, and 3075], and JP21am0101086 [0122]), by grants-in-aid from the Japan Society for the Promotion of Science (26461108, 17K09578, 18H04050, and 22H03066), and by Core Research for Evolutional Science and Technology (CREST) from the Japan Science and Technology Agency. This research was also supported by grants from the Suzuken Memorial Foundation, SENSHIN Medical Research Foundation, and the Osaka Medical Research Foundation for Intractable Diseases.

Disclosures

None.

Supplemental Material

Expanded Methods and Materials
Figures S1–S14
Tables S1–S3

REFERENCES

1. Teerlink JR, Diaz R, Felker GM, McMurray JJV, Metra M, Solomon SD, Adams KF, Anand I, Arias-Mendoza A, Biering-Sorensen T, et al; GALACTIC-HF Investigators. Cardiac myosin activation with omecamtiv mecarbil in systolic heart failure. *N Engl J Med*. 2021;384:105–116. doi: 10.1056/NEJMoa2025797
2. Psotka MA, Gottlieb SS, Francis GS, Allen LA, Teerlink JR, Adams KF Jr, Rosano GMC, Lancellotti P. Cardiac calcitropes, myotropes, and mitotropes: JACC review topic of the week. *J Am Coll Cardiol*. 2019;73:2345–2353. doi: 10.1016/j.jacc.2019.02.051
3. Felker GM, Solomon SD, Claggett B, Diaz R, McMurray JJV, Metra M, Anand I, Crespo-Leiro MG, Dahlstrom U, Goncalvesova E, et al. Assessment of omecamtiv mecarbil for the treatment of patients with severe heart failure: a post hoc analysis of data from the GALACTIC-HF randomized clinical trial. *JAMA Cardiol*. 2022;7:26–34. doi: 10.1001/jamacardio.2021.4027
4. Malik FI, Hartman JJ, Elias KA, Morgan BP, Rodriguez H, Brejc K, Anderson RL, Sueoka SH, Lee KH, Finer JT, et al. Cardiac myosin activation: a potential therapeutic approach for systolic heart failure. *Science*. 2011;331:1439–1443. doi: 10.1126/science.1200113
5. Hwang PM, Sykes BD. Targeting the sarcomere to correct muscle function. *Nat Rev Drug Discovery*. 2015;14:313–328. doi: 10.1038/nrd4554
6. Geeves MA, Holmes KC. Structural mechanism of muscle contraction. *Annu Rev Biochem*. 1999;68:687–728. doi: 10.1146/annurev.biochem.68.1.687
7. Sheikh F, Ouyang K, Campbell SG, Lyon RC, Chuang J, Fitzsimons D, Tangney J, Hidalgo CG, Chung CS, Cheng H, et al. Mouse and computational models link Mlc2v dephosphorylation to altered myosin kinetics in early cardiac disease. *J Clin Invest*. 2012;122:1209–1221. doi: 10.1172/JCI61134
8. Spudich JA. Hypertrophic and dilated cardiomyopathy: four decades of basic research on muscle lead to potential therapeutic approaches to these devastating genetic diseases. *Biophys J*. 2014;106:1236–1249. doi: 10.1016/j.bpj.2014.02.011
9. Scruggs SB, Hinken AC, Thawornkaiwong A, Robbins J, Walker LA, de Tombe PP, Geenen DL, Buttrick PM, Solaro RJ. Ablation of ventricular myosin regulatory light chain phosphorylation in mice causes cardiac dysfunction in situ and affects neighboring myofilament protein phosphorylation. *J Biol Chem*. 2009;284:5097–5106. doi: 10.1074/jbc.M807414200
10. Sanbe A, Fewell JG, Gulick J, Osinska H, Lorenz J, Hall DG, Murray LA, Kimball TR, Witt SA, Robbins J. Abnormal cardiac structure and function in mice expressing nonphosphorylatable cardiac regulatory myosin light chain 2. *J Biol Chem*. 1999;274:21085–21094. doi: 10.1074/jbc.274.30.21085
11. Toepfer CN, West TG, Ferenczi MA. Revisiting Frank-Starling: regulatory light chain phosphorylation alters the rate of force redevelopment (k_r)

in a length-dependent fashion. *J Physiol*. 2016;594:5237–5254. doi: 10.1113/JP272441
12. Colson BA, Locher MR, Bekyarova T, Patel JR, Fitzsimons DP, Irving TC, Moss RL. Differential roles of regulatory light chain and myosin binding protein-C phosphorylations in the modulation of cardiac force development. *J Physiol*. 2010;588:981–993. doi: 10.1113/jphysiol.2009.183897
13. Moss RL, Fitzsimons DP. Myosin light chain 2 into the mainstream of cardiac development and contractility. *Circ Res*. 2006;99:225–227. doi: 10.1161/01.RES.0000236793.88131.dc
14. Rottbauer W, Wessels G, Dahme T, Just S, Trano N, Hassel D, Burns CG, Katus HA, Fishman MC. Cardiac myosin light chain-2: a novel essential component of thick-myofilament assembly and contractility of the heart. *Circ Res*. 2006;99:323–331. doi: 10.1161/01.RES.0000234807.16034.fe
15. Seguchi O, Takashima S, Yamazaki S, Asakura M, Asano Y, Shintani Y, Wakeno M, Minamino T, Kondo H, Furukawa H, et al. A cardiac myosin light chain kinase regulates sarcomere assembly in the vertebrate heart. *J Clin Invest*. 2007;117:2812–2824. doi: 10.1172/JCI30804
16. Chan JY, Takeda M, Briggs LE, Graham ML, Lu JT, Horikoshi N, Weinberg EO, Aoki H, Sato N, Chien KR, et al. Identification of cardiac-specific myosin light chain kinase. *Circ Res*. 2008;102:571–580. doi: 10.1161/CIRCRESAHA.107.161687
17. Kamm KE, Stull JT. Signaling to myosin regulatory light chain in sarcomeres. *J Biol Chem*. 2011;286:9941–9947. doi: 10.1074/jbc.R110.198697
18. Ding P, Huang J, Battiprolu PK, Hill JA, Kamm KE, Stull JT. Cardiac myosin light chain kinase is necessary for myosin regulatory light chain phosphorylation and cardiac performance in vivo. *J Biol Chem*. 2010;285:40819–40829. doi: 10.1074/jbc.M110.160499
19. Warren SA, Briggs LE, Zeng H, Chuang J, Chang EI, Terada R, Li M, Swanson MS, Lecker SH, Willis MS, et al. Myosin light chain phosphorylation is critical for adaptation to cardiac stress. *Circulation*. 2012;126:2575–2588. doi: 10.1161/CIRCULATIONAHA.112.116202
20. Massengill MT, Ashraf HM, Chowdhury RR, Chrzanowski SM, Kar J, Warren SA, Walter GA, Zeng H, Kang BH, Anderson RH, et al. Acute heart failure with cardiomyocyte atrophy induced in adult mice by ablation of cardiac myosin light chain kinase. *Cardiovasc Res*. 2016;111:34–43. doi: 10.1093/cvr/cvw069
21. Hodatsu A, Fujino N, Uyama Y, Tsukamoto O, Imai-Okazaki A, Yamazaki S, Seguchi O, Konno T, Hayashi K, Kawashiri MA, et al. Impact of cardiac myosin light chain kinase gene mutation on development of dilated cardiomyopathy. *ESC Heart Failure*. 2019;6:406–415. doi: 10.1002/ehf2.12410
22. van der Velden J, Papp Z, Boontje NM, Zaremba R, de Jong JW, Janssen PM, Hasenfuss G, Stienen GJ. The effect of myosin light chain 2 dephosphorylation on Ca^{2+}-sensitivity of force is enhanced in failing human hearts. *Cardiovasc Res*. 2003;57:505–514. doi: 10.1016/s0008-6363(02)00662-4
23. Morano I. Tuning the human heart molecular motors by myosin light chains. *J Mol Med*. 1999;77:544–555. doi: 10.1007/s001099900031
24. Chang AN, Kamm KE, Stull JT. Role of myosin light chain phosphatase in cardiac physiology and pathophysiology. *J Mol Cell Cardiol*. 2016;101:35–43. doi: 10.1016/j.yjmcc.2016.10.004
25. Day SM, Tardiff JC, Ostap EM. Myosin modulators: emerging approaches for the treatment of cardiomyopathies and heart failure. *J Clin Invest*. 2022;132:e148557. doi: 10.1172/JCI148557
26. McNamara JW, Li A, Dos Remedios CG, Cooke R. The role of super-relaxed myosin in skeletal and cardiac muscle. *Biophys Rev*. 2015;7:5–14. doi: 10.1007/s12551-014-0151-5
27. Schmid M, Toepfer CN. Cardiac myosin super relaxation (SRX): a perspective on fundamental biology, human disease and therapeutics. *Biol Open*. 2021;10:bio057646. doi: 10.1242/bio.057646
28. Szczesna-Cordary D, de Tombe PP. Myosin light chain phosphorylation, novel targets to repair a broken heart?. *Cardiovasc Res*. 2016;111:5–7. doi: 10.1093/cvr/cvw098
29. Yu H, Chakravorty S, Song W, Ferenczi MA. Phosphorylation of the regulatory light chain of myosin in striated muscle: methodological perspectives. *Eur Biophys J*. 2016;45:779–805. doi: 10.1007/s00249-016-1128-z
30. Yoshimi K, Kunihiro Y, Kaneko T, Nagahora H, Voigt B, Mashimo T. ssODN-mediated knock-in with CRISPR-Cas for large genomic regions in zygotes. *Nat Commun*. 2016;7:10431. doi: 10.1038/ncomms10431
31. Shinomiya H, Kato H, Kuramoto Y, Watanabe N, Tsuruda T, Arimura T, Miyashita Y, Miyasaka Y, Mashimo T, Takuwa A, et al. Aberrant accumulation of TMEM43 accompanied by perturbed transmural gene expression in arrhythmogenic cardiomyopathy. *FASEB J*. 2021;35:e21994. doi: 10.1096/fj.202100800R
32. Higo S, Hikoso S, Miyagawa S, Sakata Y. Genome editing in human induced pluripotent stem cells (hiPSCs). *Methods Mol Biol*. 2021;2320:235–245. doi: 10.1007/978-1-0716-1484-6_21
33. Toepfer CN, Garfinkel AC, Venturini G, Wakimoto H, Repetti G, Alamo L, Sharma A, Agarwal R, Ewoldt JF, Cloonan P, et al. Myosin sequestration regulates sarcomere function, cardiomyocyte energetics, and metabolism, informing the pathogenesis of hypertrophic cardiomyopathy. *Circulation*. 2020;141:828–842. doi: 10.1161/CIRCULATIONAHA.119.042339
34. Pacher P, Nagayama T, Mukhopadhyay P, Batkai S, Kass DA. Measurement of cardiac function using pressure-volume conductance catheter technique in mice and rats. *Nat Protoc*. 2008;3:1422–1434. doi: 10.1038/nprot.2008.138
35. Hayakawa T, Kunihiro T, Ando T, Kobayashi S, Matsui E, Yada H, Kanda Y, Kurokawa J, Furukawa T. Image-based evaluation of contraction-relaxation kinetics of human-induced pluripotent stem cell-derived cardiomyocytes: correlation and complementarity with extracellular electrophysiology. *J Mol Cell Cardiol*. 2014;77:178–191. doi: 10.1016/j.yjmcc.2014.09.010
36. Kamikubo K, Tsukamoto O, Uyama-Saito Y, Oya R, Tsubota T, Fujino N, Asano Y, Kato H, Matsuoka K, Takashima S. Non-radioactive in vitro cardiac myosin light chain kinase assays. *J Vis Exp*. Published on June 23, 2020. doi: 10.3791/61168
37. Li J, Zhang L, Yu L, Minami I, Miyagawa S, Horning M, Dong J, Qiao J, Qu X, Hua Y, et al. Circulating re-entrant waves promote maturation of hiPSC-derived cardiomyocytes in self-organized tissue ring. *Commun Biol*. 2020;3:122. doi: 10.1038/s42003-020-0853-0
38. Shiba M, Higo S, Kondo T, Li J, Liu L, Ikeda Y, Kohama Y, Kameda S, Tabata T, Inoue H, et al. Phenotypic recapitulation and correction of desmoglein-2-deficient cardiomyopathy using human-induced pluripotent stem cell-derived cardiomyocytes. *Hum Mol Genet*. 2021;30:1384–1397. doi: 10.1093/hmg/ddab127
39. Mizutani H, Okamoto R, Moriki N, Konishi K, Taniguchi M, Fujita S, Dohi K, Onishi K, Suzuki N, Satoh S, et al. Overexpression of myosin phosphatase reduces Ca^{2+} sensitivity of contraction and impairs cardiac function. *Circ J*. 2010;74:120–128. doi: 10.1253/CIRCJ.cj-09-0462
40. Tobita T, Nomura S, Morita H, Ko T, Fujita T, Toko H, Uto K, Hagiwara N, Aburatani H, Komuro I. Identification of MYLK3 mutations in familial dilated cardiomyopathy. *Sci Rep*. 2017;7:17495. doi: 10.1038/s41598-017-17769-1
41. Alamo L, Pinto A, Sulbaran G, Mavarez J, Padron R. Lessons from a tarantula: new insights into myosin interacting-heads motif evolution and its implications on disease. *Biophys Rev*. 2018;10:1465–1477. doi: 10.1007/s12551-017-0292-4
42. Kampourakis T, Irving M. Phosphorylation of myosin regulatory light chain controls myosin head conformation in cardiac muscle. *J Mol Cell Cardiol*. 2015;85:199–206. doi: 10.1016/j.yjmcc.2015.06.002
43. Nag S, Trivedi DV, Sarkar SS, Adhikari AS, Sunitha MS, Sutton S, Ruppel KM, Spudich JA. The myosin mesa and the basis of hypercontractility caused by hypertrophic cardiomyopathy mutations. *Nat Struct Mol Biol*. 2017;24:525–533. doi: 10.1038/nsmb.3408
44. Karabina A, Kazmierczak K, Szczesna-Cordary D, Moore JR. Myosin regulatory light chain phosphorylation enhances cardiac beta-myosin in vitro motility under load. *Arch Biochem Biophys*. 2015;580:14–21. doi: 10.1016/j.abb.2015.06.014
45. Neumann J, Eschenhagen T, Jones LR, Linck B, Schmitz W, Scholz H, Zimmermann N. Increased expression of cardiac phosphatases in patients with end-stage heart failure. *J Mol Cell Cardiol*. 1997;29:265–272. doi: 10.1006/jmcc.1996.0271
46. van Der Velden J, Klein LJ, Zaremba R, Boontje NM, Huybregts MA, Stooker W, Eijsman L, de Jong JW, Visser CA, Visser FC, et al. Effects of calcium, inorganic phosphate, and pH on isometric force in single skinned cardiomyocytes from donor and failing human hearts. *Circulation*. 2001;104:1140–1146. doi: 10.1161/hc3501.095485
47. Avner BS, Shioura KM, Scruggs SB, Grachoff M, Geenen DL, Helseth DL Jr, Farjah M, Goldspink PH, Solaro RJ. Myocardial infarction in mice alters sarcomeric function via post-translational protein modification. *Mol Cell Biochem*. 2012;363:203–215. doi: 10.1007/s11010-011-1172-z
48. van der Velden J, Merkus D, de Beer V, Hamdani N, Linke WA, Boontje NM, Stienen GJ, Duncker DJ. Transmural heterogeneity of myofilament function and sarcomeric protein phosphorylation in remodeled myocardium of pigs with a recent myocardial infarction. *Front Physiol*. 2011;2:83. doi: 10.3389/fphys.2011.00083
49. Walker LA, Walker JS, Ambler SK, Buttrick PM. Stage-specific changes in myofilament protein phosphorylation following myocardial infarction in mice. *J Mol Cell Cardiol*. 2010;48:1180–1186. doi: 10.1016/j.yjmcc.2009.09.010

50. Fitzsimons DP, Bodell PW, Baldwin KM. Phosphorylation of rodent cardiac myosin light chain 2: effects of exercise. *J Appl Physiol.* 1989;67:2447–2453. doi: 10.1152/jappl.1989.67.6.2447
51. Toepfer CN, Sikkel MB, Caorsi V, Vydyanath A, Torre I, Copeland O, Lyon AR, Marston SB, Luther PK, Macleod KT, et al. A post-MI power struggle: adaptations in cardiac power occur at the sarcomere level alongside MyBP-C and RLC phosphorylation. *Am J Physiol Heart Circ Physiol.* 2016;311:H465–H475. doi: 10.1152/ajpheart.00899.2015
52. Swulius MT, Waxham MN. Ca^{2+}/calmodulin-dependent protein kinases. *Cell Mol Life Sci CMLS.* 2008;65:2637–2657. doi: 10.1007/s00018-008-8086-2
53. Teerlink JR, Diaz R, Felker GM, McMurray JJV, Metra M, Solomon SD, Biering-Sorensen T, Bohm M, Bonderman D, Fang JC, et al; GALACTIC-HF Investigators. Effect of ejection fraction on clinical outcomes in patients treated with omecamtiv mecarbil in GALACTIC-HF. *J Am Coll Cardiol.* 2021;78:97–108. doi: 10.1016/j.jacc.2021.04.065